Mechanobiological oscillators control lymph flow

Christian Kunert[a,1], James W. Baish[b], Shan Liao[a,2], Timothy P. Padera[a], and Lance L. Munn[a]

[a]Edwin L. Steele Laboratory, Department of Radiation Oncology, Massachusetts General Hospital and Harvard Medical School, Boston, MA 02114; and [b]Biomedical Engineering and Mechanical Engineering, Bucknell University, Lewisburg, PA 17837

Edited by Shu Chien, University of California, San Diego, La Jolla, CA, and approved July 27, 2015 (received for review April 28, 2015)

The ability of cells to sense and respond to physical forces has been recognized for decades, but researchers are only beginning to appreciate the fundamental importance of mechanical signals in biology. At the larger scale, there has been increased interest in the collective organization of cells and their ability to produce complex, "emergent" behaviors. Often, these complex behaviors result in tissue-level control mechanisms that manifest as biological oscillators, such as observed in fireflies, heartbeats, and circadian rhythms. In many cases, these complex, collective behaviors are controlled—at least in part—by physical forces imposed on the tissue or created by the cells. Here, we use mathematical simulations to show that two complementary mechanobiological oscillators are sufficient to control fluid transport in the lymphatic system: Ca^{2+}-mediated contractions can be triggered by vessel stretch, whereas nitric oxide produced in response to the resulting fluid shear stress causes the lymphatic vessel to relax locally. Our model predicts that the Ca^{2+} and NO levels alternate spatiotemporally, establishing complementary feedback loops, and that the resulting phasic contractions drive lymph flow. We show that this mechanism is self-regulating and robust over a range of fluid pressure environments, allowing the lymphatic vessels to provide pumping when needed but remain open when flow can be driven by tissue pressure or gravity. Our simulations accurately reproduce the responses to pressure challenges and signaling pathway manipulations observed experimentally, providing an integrated conceptual framework for lymphatic function.

lymphatic | mechanobiology | computational model | control | biological oscillator

Flow of fluid within the lymphatic system is central to many aspects of physiology, including fluid homeostasis and immune function, and poor lymphatic drainage results in significant morbidity in millions of patients each year (1). Although it is known that various mechanical and chemical perturbations can affect lymphatic pumping, there are still no pharmacological therapies for lymphatic pathologies. A fundamental understanding of how various signals coordinate lymphatic vessel function is a necessary first step toward development of treatments to restore fluid balance and enhance immunosurveillance.

The lymphatic system consists of fluid-absorbing initial lymphatic vessels that converge to collecting lymphatic vessels, which transport lymph through lymph nodes and back to the blood circulation (2). The collecting lymphatic vessels actively transport fluid via contractions of their muscle-invested walls. Unidirectional flow is achieved by intraluminal valves that limit back flow. Unfortunately, lymphatic pumping is not always operational, and this can lead to lymphedema and immune dysfunction (3, 4).

Much is known about the mechanisms responsible for the contractions of the vessel wall. As in blood vessels, the muscle cells that line lymphatic vessels respond to changes in Ca^{2+} concentration. Membrane depolarization results in an influx of Ca^{2+} to initiate the contractions, and this process can be modulated by neurotransmitters (5) or inflammatory mediators, which generally alter the frequency and amplitude of lymphatic pumping (4, 6). Many studies have also reported that physical distension, either by applying isometric stretch or by pressurizing the vessel can affect the phasic contractions (7–10). Interestingly, endothelial (11) and smooth muscle cells (12) have stretch-activated ion channels that can initiate Ca^{2+} mobilization in response to mechanical stresses. Thus, stretch may constitute an important trigger for the contraction phase of a pumping cycle.

There are also complementary mechanisms for tempering the Ca^{2+}-dependent contractions. The most notable is nitric oxide (NO), a vasodilator that acts at multiple points in the Ca^{2+}-contraction pathway to modulate Ca^{2+} release and uptake, as well as the enzymes responsible for force production (13). Blocking or enhancing NO activity can dramatically affect pumping behavior (4, 14–17). Furthermore, lymphatic endothelial cells produce NO in response to fluid flow (16, 18, 19). Importantly, NO dynamics are faster than observed pumping frequencies, so flow-induced NO production is another potential mechanosignal involved in lymphatic regulation (20).

Model Formulation

We hypothesized that Ca^{2+} and NO cooperate to control lymphatic transport via mechanobiological feedback loops: during a lymphatic contraction cycle, increased shear causes local endothelial NOS (eNOS) activation, and the subsequent production of NO results in blunting and/or reversal of the Ca^{2+}-dependent contraction. As the vessel relaxes, NO degrades rapidly and its production drops due to the reduced fluid velocity in the now larger-diameter vessel. Meanwhile membrane potentials and resting calcium levels are restored in preparation for another contraction. The next contraction can be triggered by any signal able to initiate the Ca^{2+} mobilization, including opening of stretch-activated channels, neurotransmitters, or Ca^{2+} flux through gap junctions of neighboring cells (Fig. 1*A*).

Significance

Dysfunction of lymphatic drainage results in significant morbidity in millions of patients each year, and there are currently no pharmacological treatments available. Because a mechanistic understanding of lymphatic control has been elusive, it has not been possible to develop effective, targeted therapies to alleviate lymphedema or facilitate immune cell trafficking in lymphatic pathologies. Here, we show that complementary biological oscillators control lymphatic transport, driven by mechanosensitive calcium and nitric oxide (NO) dynamics. The mechanism shows fascinating adaptability and autoregulation, inducing active pumping of the lymphatic vessels when gravity opposes flow, but vessel relaxation when pressures are able to drive flow passively.

Author contributions: C.K., J.W.B., T.P.P., and L.L.M. designed research; C.K. and S.L. performed research; C.K. developed mathematical model and performed numerical simulations; S.L., T.P.P., and L.L.M. contributed new reagents/analytic tools; C.K., J.W.B., T.P.P., and L.L.M. analyzed data; and C.K., J.W.B., S.L., T.P.P., and L.L.M. wrote the paper.

The authors declare no conflict of interest.

This article is a PNAS Direct Submission.

Freely available online through the PNAS open access option.

[1]To whom correspondence should be addressed. Email: kuni@steele.mgh.harvard.edu.

[2]Present address: Department of Microbiology, Immunology and Infectious Diseases, Snyder Institute for Chronic Diseases, Cumming School of Medicine, University of Calgary, Calgary, AB, Canada T2N 1N4.

This article contains supporting information online at www.pnas.org/lookup/suppl/doi:10.1073/pnas.1508330112/-/DCSupplemental.

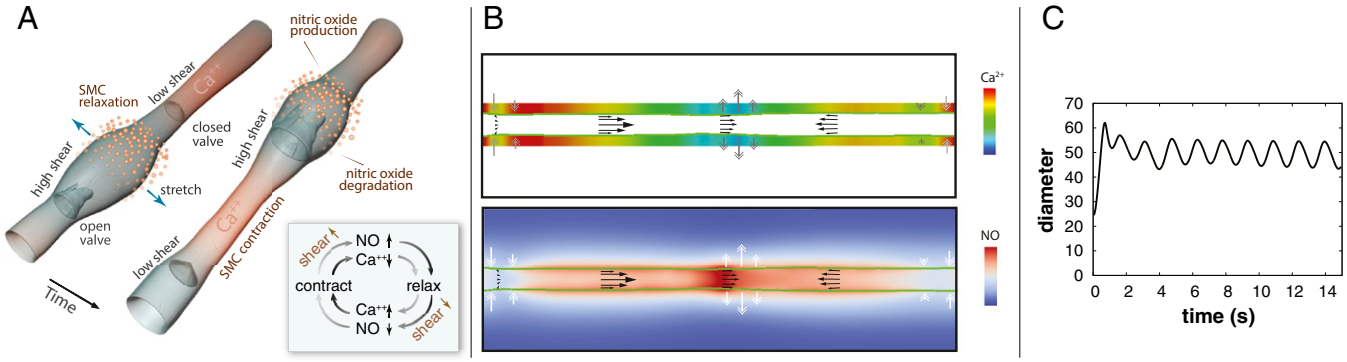

Fig. 1. Dynamics of lymphatic pumping. (*A*) Conceptual scheme, showing two different snapshots of cyclic lymphatic pumping. Flow direction is from *Bottom Left* to *Top Right*. Nitric oxide relaxes the vessel wall, increasing vessel diameter and pulling fluid from upstream. As the lymphangion fills, the upstream valve is open, and the downstream valve is closed. When the lymphangion is filled, flow and shear stress decrease, and NO is degraded; a subsequent contraction can be initiated through Ca^{2+} influx via stretch-, voltage-, or ion-activated channels. The contraction closes the upstream valve and opens the downstream valve, increases wall shear stress, and induces NO production locally, thus starting the cycle again (NO: orange; cytosolic Ca^{2+}: red). Depending on the biochemical and fluid environment, this basic mechanism can be tuned to produce various frequencies and amplitudes. (*B*) Snapshot of the simulated system. The vessel boundary is indicated by the green line. Instantaneous Ca^{2+} and NO concentrations are shown in the *Top* and *Bottom* color maps, respectively. The flow field is represented by the black arrows, and the current wall velocity is shown in the gray/white double arrows. Valves are located at each end, and at center. (*C*) Pumping dynamics predicted by the model. At $t = 0$, flow is initiated by a mechanical perturbation. The system quickly stabilizes and subsequent pumping is self-sustained.

To test whether this scheme is sufficient to produce the complex behaviors observed for lymphatic vessels in experiments, we created a multiscale, mechanistic mathematical model. The underlying assumptions of the model are based on well-documented experimental findings as follows: (*i*) Lymphatic contractions are mediated by Ca^{2+} influx in the lymphatic muscle cell cytosol, which culminates in myosin light chain phosphorylation and induction of the myosin–actin cross-bridges (6, 21–23) (*Supporting Information*). (*ii*) The lymphatic muscle contractile force increases with cytosolic Ca^{2+} concentration (with saturating kinetics); the maximum possible force decreases with the radius (to reproduce the known length–force relationship) (22–26). (*iii*) Ca^{2+} accumulates in the cytosol at a constant, slow rate (i.e., influx through T-type channels) (23, 27, 28) and is depleted via ion pumps (23, 29). (*iv*) Pressurizing or stretching the vessel can enhance Ca^{2+} influx (stretch-activated channels) (5, 7, 30). (*v*) Accumulation of cytosolic Ca^{2+} in excess of a threshold concentration induces a rapid influx of Ca^{2+} (reproducing influx into L-type channels and Ca^{2+}-induced Ca^{2+} release) (5, 6, 23, 28, 30, 31). (*vi*) Ca^{2+} diffuses through gap junctions to adjacent lymphatic muscle cells (32–34). (*vii*) NO can deplete cytosolic Ca^{2+} and decrease its rate of accumulation (35–37). (*viii*) NO is produced by endothelium when shear stress exceeds a threshold value (16, 38–40). (*ix*) NO diffuses and advects, and has a half-life on the order of 1 s (20). (*x*) The vessel contains intraluminal valves that inhibit backflow and also act as sources of NO (16, 38, 41).

We solve the lymph flow field using the lattice Boltzmann method (42). Moving boundaries are implemented by exchanging momentum at each boundary node with the fluid (43), and the movement of each boundary node is calculated locally by Verlet integration.

The Ca^{2+} dynamics are calculated by solving a system of differential equations, based on the local vessel radius and NO concentration. NO is produced in the vessel boundary and at the valves by lymphatic endothelial cells. NO acts upon nearby lymphatic muscle cells that wrap around the vessel and are responsible for the contractions (in low NO concentrations) and dilations (in high NO concentrations). Details of the model formulation are described in *Supporting Information*.

Results

In the simulations, an initial perturbation causes the vessel to produce self-sustained, cyclic contractions (Fig. 1 *B* and *C*). The walls move with a characteristic frequency determined by the Ca^{2+} and NO kinetics, the fluid pressure, and the wall mechanics (*Supporting Information* and Movie S1). The mechanobiological feedback causes complementary oscillations in Ca^{2+} and NO concentrations. Experimentally, oscillations in Ca^{2+} were identified decades ago (44), whereas the corresponding variation in NO concentration was reported more recently (16, 38). These studies found that the NO concentration varies spatially along the vessel, but also temporally during the contraction cycle, as predicted by the simulations (Fig. 1*B* and Movies S1–S4).

There are many experimental approaches to test the proposed theory of lymphatic control. The most relevant experiments are those that challenge the system with physiological perturbations that an actual lymphatic vessel would experience in vivo and determine whether the response of the model is appropriate. Therefore, we first tested whether the model can reproduce the results of experiments in mice under baseline conditions and with inflammation. Under normal conditions, phasic contractions in vivo can adopt various amplitudes and frequencies: low-frequency, high-amplitude "strong" pumping, and higher-frequency, lower-amplitude "weak" pumping are typical (Fig. 2*A*) (4). However, when mice were treated with oxazolone to induce inflammation (4), strong and weak pumping were observed, but a third behavior also appeared—highly dilated vessels with little vasomotion (Fig. 2*B*). This behavior was likely due to elevated tissue pressure driving flow through the vessel.

In the simulations, we were able to reproduce these behaviors by imposing the physiologically appropriate pressure conditions and baseline diameters. For axial pressures, negative gradients drive flow through the vessel while positive gradients oppose the flow. Applying a moderate axial driving pressure (−10) reproduced weak pumping seen under physiological conditions in the mouse (Fig. 2*C*, red line). Introducing an opposing pressure gradient (+20) increased the contraction amplitude, similar to the strong pumping case in vivo (Fig. 2*C*, blue line). To simulate inflammation, the baseline diameter was increased to provide an overall decrease in tone, and then various pressure conditions were applied (Fig. 2*D*). An opposing pressure gradient (+40) produced large-amplitude pumping as before (blue line), and smaller amplitude pumping was seen with no pressure gradient (red line). Pressure-driven flow (−14) resulted in an open, noncontractile vessel due to high NO production (Fig. 2*D*, black line). This case simulated leakage of fluid from blood vessels and transmission of

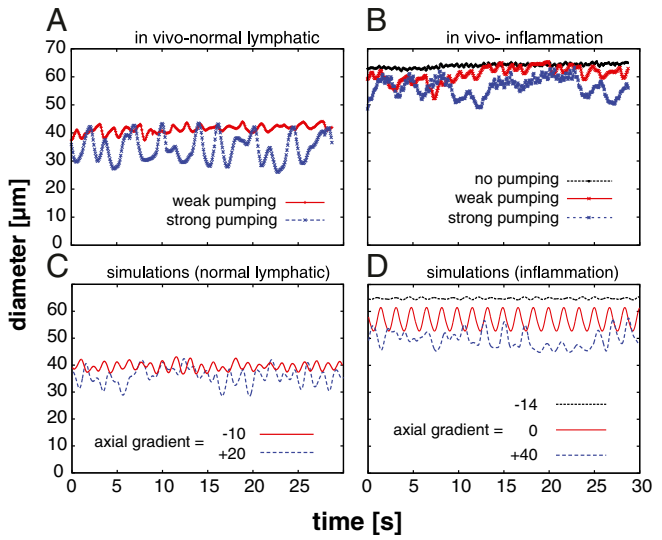

Fig. 2. Multiple pumping behaviors predicted by simulations and observed in vivo (Movies S1–S4). (*A*) Lymphatic contractions in the mouse hindlimb model occur with a range of frequencies and amplitudes. High-amplitude, low-frequency strong pumping (blue), and lower-amplitude, higher-frequency weak pumping (red) are seen in the collecting lymphatic vessel feeding the popliteal lymph node in C57BL/6 mice (plots are from intravital microscopy of the same mouse at different times). (*B*) In addition to strong and weak pumping, vessels can dilate and minimize contractions (black line) in response to inflammation induced by oxazolone skin painting. (*C*) Strong (blue) and weak pumping (red) are reproduced in the simulations by varying the axial pressure gradient. (*D*) To simulate the multiple behaviors during inflammation, only the baseline diameters and pressure gradient were adjusted. The large-diameter mode with no contractions can be reproduced in the simulations by imposing a driving axial pressure gradient, which induces shear stress, producing NO and maintaining relaxation (black).

pressure to the initial lymphatic vessels—common conditions in inflammation—which help to drive the flow. Note that it was not necessary to reformulate the model or adjust multiple parameters to produce these various behaviors. They emerged naturally due to the mechanobiological feedback in the various pressure environments.

Another approach to test the model is to pharmacologically or genetically disrupt the Ca^{2+}–NO oscillator and see whether the predictions of the theory match experimental observations. Many experiments have shown that blocking NO production has dramatic effects on contractions. This has been done using pharmacological inhibitors (45) and genetically modified mice (4, 45), and by denuding the endothelium to remove the source of NO (46, 47). In experiments with eNOS-deficient mice, contractions are inhibited when the lymphatics are studied in situ (4), but the vessel can be induced to pump by pressurizing the lumen in ex vivo preparations (46, 47). Thus, there is apparently a deficiency introduced by the lack of NO that can be restored by pressurizing the lumen. In our simulations, we can deactivate NO to investigate this question. Without NO production, phasic contractions are inhibited and can only occur at moderate transwall pressures, which are capable of providing the stretch-activated Ca^{2+} spikes (Fig. 3*A*, green). With lower pressures, insufficient stretch activation occurs (red). At higher pressures, the stretch channels are always activated, resulting in stasis (purple). Thus, it is possible for the Ca^{2+} oscillations to occur without NO steering if the fluid pressure and wall mechanics are balanced.

To further examine the role of NO in controlling the phasic contractions, we reactivated it in the model. In these simulations, there is consistent pumping over a wide range of transwall pressures, as well as a decrease in vessel tone (larger diameter) due to cooperation between the pressure-induced stretch and NO-mediated relaxation (Fig. 3*B*). Thus, NO signaling allows contractions to occur over a wider range of transmural pressures, establishing a more robust transport system.

Interestingly, the performance of the system is affected by the kinetics of the shear-induced signaling species. If this signal has a short lifetime, lymphangion filling is insufficient, whereas with longer lifetimes, pumping frequency slows (Fig. 3*C*). The actual lifetime of NO depends on local oxygen concentration, but is in the range of 0.1–1 s (20), corresponding to the optimum in

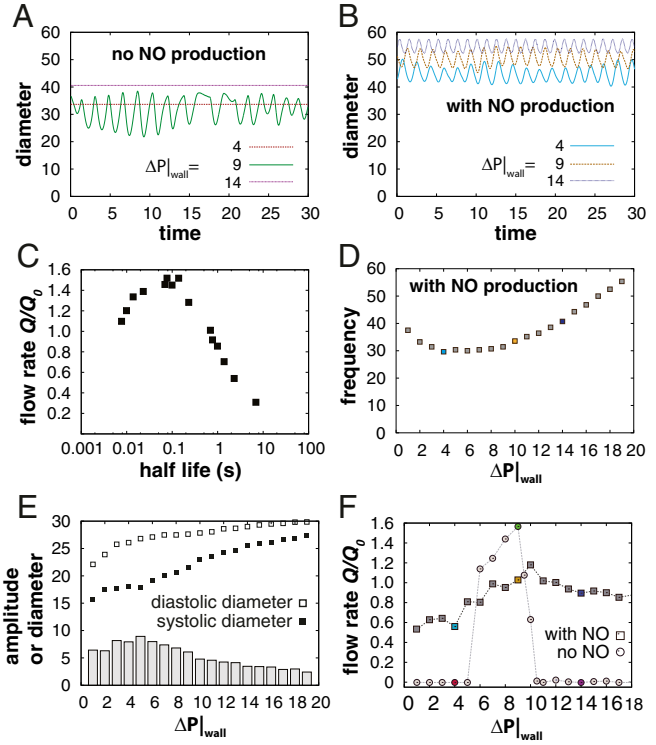

Fig. 3. Ca^{2+} and NO cooperate to optimize lymph transport (simulations). (*A*) Simulations without NO activity. At low transwall pressure $\Delta P|_{wall}$, vessel stretch is insufficient to induce Ca^{2+} contractions (red). High pressures stop contractions (purple). At moderate pressures, Ca^{2+} can mediate pumping without NO (green). The axial pressure gradient was zero for all three simulations. (*B*) Modulation of the Ca^{2+} mechanism by NO. The simulations in *A* were repeated, but with shear-induced NO present. The system pumps at all three pressures. (*C*) Signaling species kinetics is important. To achieve efficient transport, the shear-induced steering molecule should have a half-life on the order of 0.01–1 s. (*D*) The changes in frequency with pressure are inversely proportional to the amplitude due to the longer distance a boundary point has to travel. Low transwall pressures result in smaller diastolic diameters, and correspondingly smaller amplitude. High transwall pressures, on the other hand, limit the systolic diameter, also reducing amplitudes. The light blue, gold, and dark blue data points correspond to the traces in *B*. (*E*) Diastolic and systolic diameters (squares)—and the contraction amplitude (gray bars)—are affected by transwall pressure $\Delta P|_{wall}$. For high pressures, both approach the same limit, determined by the mechanical properties of the wall. For low pressures, the vessel cannot fully relax, because the pressure does not provide sufficient opening force. At moderate pressures, the fluid can dilate the vessel, but the lymphatic muscle cells can overcome the fluid pressure; amplitude is maximized in this regime. (*F*) NO improves flow at high and low transwall pressures. Simulations were performed with no axial pressure gradient. With low transwall pressure, no pumping occurs without NO (circles). At high pressure, contraction amplitude is limited, and again, flow is negligible. At intermediate pressures, stretch-induced contractions and Ca^{2+} oscillations can drive flow. Note that the range of pressures where Ca^{2+} can operate independently is relatively narrow. With NO, flow rates are more consistent over the range of pressures. The colored data points correspond to the respective traces in *A* and *B*.

our simulations (Fig. 3*C*). Note that other endothelial-derived relaxation factors, such as histamine (48), generally have much longer lifetimes and would not be able to drive the oscillations.

We next investigated further the relationship between transwall pressure and pumping performance. Because it is possible to precisely control vascular pressure in ex vivo lymphatic studies, there is a rich literature investigating the effect of transwall pressure on vessel contractions (8, 28, 49–54). In these experiments, there is a monotonic increase in pumping frequency with pressure, but a peak in amplitude at a moderate pressures (28, 49, 50). In agreement with these observations, our simulations (with NO active) show an increase in frequency with pressure from a minimum at $\Delta P|_W \sim 6$ (Fig. 3*D*). We also reproduce the peak in amplitude that is observed in experiments, but previously unexplained. According to our simulations, this is due to a rapid increase in diastolic diameter with pressure while the systolic diameter lags behind (Fig. 3*E*). The system is able to perform without NO, but only over a small window of transwall pressures (Fig. 3*F*).

In addition to transwall pressures, lymphatic vessels can also experience intraluminal pressure gradients along the vessel axis that can affect flow. In experimental studies conducted by controlling flow through cannulated ex vivo lymphatic preparations, contractions are affected by axial pressure gradients that either drive flow through the vessel (negative gradient) or force the vessel to pump against pressure (positive gradient) (52, 55–60). In these experiments, imposed flow tends to inhibit contractions, and our simulations reproduce this behavior, predicting decreasing amplitude with increasingly negative (helping) axial pressures (Fig. 4*A*). At sufficiently high imposed flow, contractions are completely inhibited as NO quenches the Ca^{2+}-induced contractions (Fig. 4*A*, $\delta P/\delta x$ less than approximately −12). Without the contractions, which increase flow resistance, there is a linear increase in flow rate with increasingly negative axial pressures (Fig. 4*B*, with NO).

The advantage of a computational model is that we can challenge the system with a variety of physiological conditions and observe the performance, which is best measured by the output flow rate of the vessel. With NO, the flow is relatively constant, even as the opposing pressure gradient increases (Fig. 4*B*; squares, pressure gradient > 0). The normalized flow rate $Q^* = Q/Q_0$ drops from $Q^* = 1.0$ at $\delta P/\delta x = 0$ to $Q^* = 0.72$ at $\delta P/\delta x = 10$ to $Q^* = 0.50$ at $\delta P/\delta x = 20$. As the pressure gradient becomes negative (driving flow), NO damps the contractions, relaxing the vessel and allowing pressure-driven flow (squares, axial pressure gradient less than −10). Without NO, the performance of the lymphatic contraction is highly dependent on the transwall pressure. For a transwall pressure of 9 (Fig. 4*B*, circles), Ca^{2+} oscillations alone can drive the pumping due to stretch-induced Ca^{2+} fluctuations. At this transwall pressure, the performance is slightly better ($Q^* = 1.60$ at $\delta P/\delta x = 0$) than the case with active NO signaling, as NO inhibits the Ca^{2+}-dependent contractions. However, without NO, the vessel continues to pump even when negative pressure is available to drive the flow, and this increases resistance, lowering the output (at $\delta P/\delta x = 20$, $Q^* = 2.66$ without NO vs. $Q^* = 7.58$ with NO). Increasing the transwall pressure slightly from $P|_{wall} = 9$ to $P|_{wall} = 10$ results in consistently lower flow rates compared with the case with NO production (triangles), and there is only a small window of transwall pressures in which the Ca^{2+} can mediate pumping independent of NO (Fig. 3*F*). With no axial pressure gradient, NO-independent pumping can occur for moderate transwall pressures. At lower transwall pressures, there is insufficient stretch activation of Ca^{2+}, whereas at higher transwall pressures, the contractions cannot overcome the fluid pressure. In these regimes, the NO dynamics can control the pumping, leading to a nonzero flow rate over a large range (squares).

We emphasize that there were no changes made to the model formulation to reproduce the experimental findings described above. Except for the activation/deactivation of NO, only the boundary conditions that dictate the fluid pressure environment (and in the case of inflammation, the baseline diameter) were changed to match the data. Thus, all these behaviors emerge naturally from the nonlinear dynamics of the Ca^{2+}–NO mechanism.

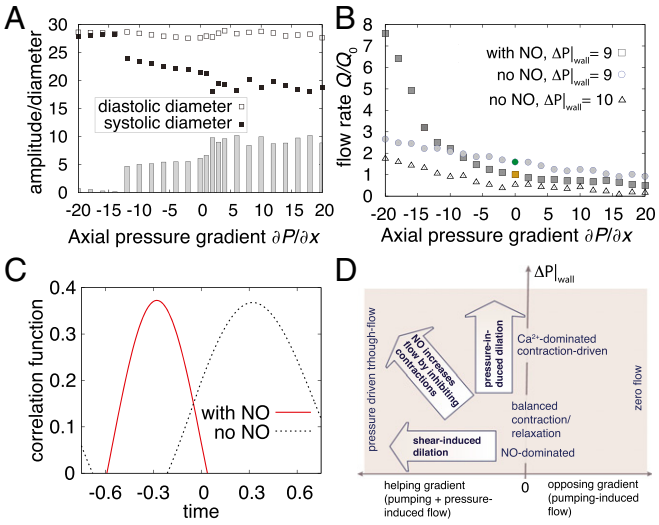

Fig. 4. Influence of axial pressure gradients and overall performance (simulations). (*A*) Systolic and diastolic diameters are affected by axial pressure gradient. $\Delta P|_{wall} = 9$ for these simulations. Although the diastolic diameter varies little, the systolic diameter adapts to the imposed pressure. At large negative (driving) pressures, NO inhibits contractions. Otherwise, NO coordinates the contractions to drive flow. The gray bars show the corresponding amplitudes. (*B*) Flow rates are improved by NO steering. With $\Delta P|_{wall} = 9$, flow is slightly better without NO production with opposing (positive) and neutral pressure gradients compared with the case with NO (circles vs. squares, positive pressure gradient). With negative pressure gradients (driven flow), shear-induced NO relaxes the vessel, reducing flow resistance (squares, negative pressure gradients). In this regime without NO ($\Delta P|_{wall} = 9$), the vessel continues to contract even when pressure-driven flow is present, and this increases flow resistance. The simulations without NO at $\Delta P|_{wall} = 9$ represent the optimum case: Slightly increasing the transwall pressure to 10 results in consistently less output over the range of axial pressures (triangles). The colored data points correspond to the respective simulations in Fig. 3 *A* and *B*. (*C*) Contraction wave propagation. To quantify the direction of propagation of the contractions, we calculated the cross-correlation function of the radius over time at two nearby points in the vessel wall. With shear-induced NO, there is a backward propagation of the contractions (red, negative time shift); without NO, the contractions propagate forward (black, positive time shift). (*D*) Behavior map of transport in a collecting lymphatic vessel. The performance of the system is summarized as a function of axial (*x* axis) and transwall (*y* axis) pressure gradients.

A previously unexplained experimental observation concerns the apparent direction of propagation of the lymphatic contractions along the vessel. Zawieja et al. (61, 62) reported that the majority of the contraction waves are either static or in the direction opposite to the flow. This counterintuitive finding suggested that lymphatic contractions do not operate via conventional peristalsis but are coordinated by mechanisms that can travel upstream. However, researchers have yet to identify such signals. Indeed, blocking the prime candidates—gap junctions—reduces the pumping by ∼30% but does not stop the cyclic contractions (28). To investigate this anomaly, we performed larger simulations with eight lymphangions to more easily observe the direction of propagation. We found that the direction depends on whether NO or Ca^{2+} is dominating the system. When NO dominates, we observe retrograde propagation of the contraction wave. In contrast, when Ca^{2+} dominates, the contractions propagate in the forward direction (Fig. 4*C* and Movies S5 and S6). This behavior is likely due to the ability of the vessel to

"pull" fluid from upstream when the NO mechanism actively dilates the vessel, whereas when Ca^{2+} dominates, the fluid is predominately "pushed" downstream by the Ca^{2+}-induced contractions.

Discussion

The transduction of mechanical signals is prevalent in biology, and research in this area is accelerating (63–67). The mechanobiological control mechanisms described here result in a robust transport system that adapts to varying fluid environments to optimize lymph transport while minimizing metabolic costs (Fig. 4*D*). It automatically reacts to changes in tissue fluid pressures, adjusting vasomotion as needed for lymph clearance. Mechanobiological feedback also makes lymphatics energy-efficient, contracting only when needed.

Although it accurately reproduces the robust and versatile activity of lymphatic vessels, our model does not encompass all of the regulatory control of lymphatic vessel function, and there are likely additional mechanisms that can control vessel tone, independent of the pumping mechanism (68–70). Nevertheless, the model suggests that shear-driven NO feedback enables lymph transport over a range of transwall and axial pressure gradient conditions not possible in the absence of NO signaling. Thus, any malfunction in the endothelial mechanosensory machinery or downstream pathways that produce NO could result in impaired lymphatic transport. Similarly, excess production of NO by tissue cells can obfuscate the NO oscillations and interfere with the pumping (4). Modulation of these components in the clinic may lead to better therapies for lymphedema and weakened immune responses.

The biological feedback mechanism described here is an important example of emergent behavior and biological oscillation. Following simple, local mechanisms, a collection of cells in the vessel wall can produce amazingly complex, coordinated, and appropriate behavior. The identification of the oscillating system driven by NO and Ca^{2+} dynamics provides a unified theory able to explain many key features of lymphatic physiology: how lymphatic vessels respond appropriately to changes in pressure gradients and transwall pressures, how underproduction or overproduction of NO can interfere with pumping, and even why the propagation of wall contractions can oppose the flow direction. In the context of this theory, no additional chemical or electrical signals are necessary—the mechanobiological signals of fluid shear stress and mechanical stretch provide sufficient feedback to coordinate the contractions. From the perspective of control theory, the oscillator constitutes a closed-loop system, capable of interesting and diverse behaviors. In the simulations, and in experiments, removing the NO mechanism effectively disrupts the loop and reduces the system to one dependent only on Ca^{2+} dynamics. Further analysis of this control system should reveal additional strategies for shifting its output to either increase or decrease lymph flow for therapeutic purposes. It remains to be seen whether this mechanism is present in other aspects of vascular biology, but its robust nature suggests that it may play a role in other systems requiring variable demand for fluid transport such as vasomotion in the blood vasculature or during development of the cardiovascular system, before neuronal control is established.

Methods

All procedures were performed following the guidelines of the Institutional Animal Care and Use Committee of the Massachusetts General Hospital.

ACKNOWLEDGMENTS. We thank Drs. Jonathan Song and Dennis Jones for unpublished studies that guided this project. This work was funded in part by National Institutes of Health Grants R01-CA149285 (to L.L.M.), R00-CA137167, R21-AI097745, and DP2-OD008780 (to T.P.P.), R01-HL128168 (to J.W.B., T.P.P., and L.L.M.), and Deutsche Forschungsgemeinschaft Grant Ku 2909/1 (to C.K.).

1. Brorson H, Ohlin K, Olsson G, Svensson B, Svensson H (2008) Controlled compression and liposuction treatment for lower extremity lymphedema. *Lymphology* 41(2): 52–63.
2. Mendoza E, Schmid-Schönbein GW (2003) A model for mechanics of primary lymphatic valves. *J Biomech Eng* 125(3):407–414.
3. Elias RM, Johnston MG, Hayashi A, Nelson W (1987) Decreased lymphatic pumping after intravenous endotoxin administration in sheep. *Am J Physiol* 253(6 Pt 2): H1349–H1357.
4. Liao S, et al. (2011) Impaired lymphatic contraction associated with immunosuppression. *Proc Natl Acad Sci USA* 108(46):18784–18789.
5. Zhao J, van Helden DF (2003) ET-1-associated vasomotion and vasospasm in lymphatic vessels of the guinea-pig mesentery. *Br J Pharmacol* 140(8):1399–1413.
6. von der Weid PY (2001) Review article: Lymphatic vessel pumping and inflammation—the role of spontaneous constrictions and underlying electrical pacemaker potentials. *Aliment Pharmacol Ther* 15(8):1115–1129.
7. Shirasawa Y, Benoit JN (2003) Stretch-induced calcium sensitization of rat lymphatic smooth muscle. *Am J Physiol Heart Circ Physiol* 285(6):H2573–H2577.
8. McHale NG, Roddie IC (1976) The effect of transmural pressure on pumping activity in isolated bovine lymphatic vessels. *J Physiol* 261(2):255–269.
9. Davis MJ, et al. (2012) Intrinsic increase in lymphangion muscle contractility in response to elevated afterload. *Am J Physiol Heart Circ Physiol* 303(7):H795–H808.
10. Scallan JP, Wolpers JH, Davis MJ (2013) Constriction of isolated collecting lymphatic vessels in response to acute increases in downstream pressure. *J Physiol* 591(Pt 2): 443–459.
11. Lansman JB, Hallam TJ, Rink TJ (1987) Single stretch-activated ion channels in vascular endothelial cells as mechanotransducers? *Nature* 325(6107):811–813.
12. Davis MJ, Donovitz JA, Hood JD (1992) Stretch-activated single-channel and whole cell currents in vascular smooth muscle cells. *Am J Physiol* 262(4 Pt 1):C1083–C1088.
13. Barouch LA, et al. (2002) Nitric oxide regulates the heart by spatial confinement of nitric oxide synthase isoforms. *Nature* 416(6878):337–339.
14. Shirasawa Y, Ikomi F, Ohhashi T (2000) Physiological roles of endogenous nitric oxide in lymphatic pump activity of rat mesentery in vivo. *Am J Physiol Gastrointest Liver Physiol* 278(4):G551–G556.
15. von der Weid PY, Zhao J, Van Helden DF (2001) Nitric oxide decreases pacemaker activity in lymphatic vessels of guinea pig mesentery. *Am J Physiol Heart Circ Physiol* 280(6):H2707–H2716.
16. Bohlen HG, Gasheva OY, Zawieja DC (2011) Nitric oxide formation by lymphatic bulb and valves is a major regulatory component of lymphatic pumping. *Am J Physiol Heart Circ Physiol* 301(5):H1897–H1906.
17. Gasheva OY, Zawieja DC, Gashev AA (2006) Contraction-initiated NO-dependent lymphatic relaxation: A self-regulatory mechanism in rat thoracic duct. *J Physiol* 575(Pt 3):821–832.
18. Shyy JYJ, Chien S (2002) Role of integrins in endothelial mechanosensing of shear stress. *Circ Res* 91(9):769–775.
19. Kuchan MJ, Frangos JA (1994) Role of calcium and calmodulin in flow-induced nitric oxide production in endothelial cells. *Am J Physiol* 266(3 Pt 1):C628–C636.
20. Thomas DD, Liu X, Kantrow SP, Lancaster JR, Jr (2001) The biological lifetime of nitric oxide: Implications for the perivascular dynamics of NO and O_2. *Proc Natl Acad Sci USA* 98(1):355–360.
21. Lee J, Ishihara A, Oxford G, Johnson B, Jacobson K (1999) Regulation of cell movement is mediated by stretch-activated calcium channels. *Nature* 400(6742):382–386.
22. Wang W, et al. (2009) Inhibition of myosin light chain phosphorylation decreases rat mesenteric lymphatic contractile activity. *Am J Physiol Heart Circ Physiol* 297(2): H726–H734.
23. Karaki H, et al. (1997) Calcium movements, distribution, and functions in smooth muscle. *Pharmacol Rev* 49(2):157–230.
24. Dougherty PJ, et al. (2014) PKC activation increases Ca^{2+} sensitivity of permeabilized lymphatic muscle via myosin light chain 20 phosphorylation-dependent and -independent mechanisms. *Am J Physiol Heart Circ Physiol* 306(5):H674–H683.
25. Murphy RA, Walker JS (1998) Inhibitory mechanisms for cross-bridge cycling: The nitric oxide-cGMP signal transduction pathway in smooth muscle relaxation. *Acta Physiol Scand* 164(4):373–380.
26. Harris DE, Warshaw DM (1991) Length vs. active force relationship in single isolated smooth muscle cells. *Am J Physiol* 260(5 Pt 1):C1104–C1112.
27. Major TC, et al. (2008) The T- and L-type calcium channel blocker (CCB) mibefradil attenuates leg edema induced by the L-type CCB nifedipine in the spontaneously hypertensive rat: A novel differentiating assay. *J Pharmacol Exp Ther* 325(3):723–731.
28. Lee S, Roizes S, von der Weid PY (2014) Distinct roles of L- and T-type voltage-dependent Ca2+ channels in regulation of lymphatic vessel contractile activity. *J Physiol* 592(Pt 24):5409–5427.
29. Clapham DE (2007) Calcium signaling. *Cell* 131(6):1047–1058.
30. Laver DR, Kong CH, Imtiaz MS, Cannell MB (2013) Termination of calcium-induced calcium release by induction decay: An emergent property of stochastic channel gating and molecular scale architecture. *J Mol Cell Cardiol* 54:98–100.
31. Collier ML, Ji G, Wang Y, Kotlikoff MI (2000) Calcium-induced calcium release in smooth muscle: Loose coupling between the action potential and calcium release. *J Gen Physiol* 115(5):653–662.
32. Aalkjær C, Boedtkjer D, Matchkov V (2011) Vasomotion—what is currently thought? *Acta Physiol (Oxf)* 202(3):253–269.

33. Kapela A, Parikh J, Tsoukias NM (2012) Multiple factors influence calcium synchronization in arterial vasomotion. *Biophys J* 102(2):211–220.
34. Meens MJ, Sabine A, Petrova TV, Kwak BR (2014) Connexins in lymphatic vessel physiology and disease. *FEBS Lett* 588(8):1271–1277.
35. Kannan MS, Prakash YS, Johnson DE, Sieck GC (1997) Nitric oxide inhibits calcium release from sarcoplasmic reticulum of porcine tracheal smooth muscle cells. *Am J Physiol* 272(1 Pt 1):L1–L7.
36. Heunks LM, Cody MJ, Geiger PC, Dekhuijzen PN, Sieck GC (2001) Nitric oxide impairs Ca^{2+} activation and slows cross-bridge cycling kinetics in skeletal muscle. *J Appl Physiol (1985)* 91(5):2233–2239.
37. Kapela A, Bezerianos A, Tsoukias NM (2008) A mathematical model of Ca^{2+} dynamics in rat mesenteric smooth muscle cell: Agonist and NO stimulation. *J Theor Biol* 253(2): 238–260.
38. Bohlen HG, Wang W, Gashev A, Gasheva O, Zawieja D (2009) Phasic contractions of rat mesenteric lymphatics increase basal and phasic nitric oxide generation in vivo. *Am J Physiol Heart Circ Physiol* 297(4):H1319–H1328.
39. Rahbar E, Akl T, Coté GL, Moore JE, Jr, Zawieja DC (2014) Lymph transport in rat mesenteric lymphatics experiencing edemagenic stress. *Microcirculation* 21(5): 359–367.
40. Nagai T, Bridenbaugh EA, Gashev AA (2011) Aging-associated alterations in contractility of rat mesenteric lymphatic vessels. *Microcirculation* 18(6):463–473.
41. Schmid-Schönbein GW (1990) Microlymphatics and lymph flow. *Physiol Rev* 70(4): 987–1028.
42. Succi S (2001) *The Lattice Boltzmann Equation for Fluid Dynamics and Beyond* (Oxford Univ Press, Oxford).
43. Verberg R, Ladd AJC (2002) Accuracy and stability of a lattice-Boltzmann model with subgrid scale boundary conditions. *Phys Rev E Stat Nonlin Soft Matter Phys* 65(1 Pt 2): 016701.
44. Azuma T, Ohhashi T, Sakaguchi M (1977) Electrical activity of lymphatic smooth muscles. *Proc Soc Exp Biol Med* 155(2):270–273.
45. Hagendoorn J, et al. (2004) Endothelial nitric oxide synthase regulates microlymphatic flow via collecting lymphatics. *Circ Res* 95(2):204–209.
46. Gashev AA, et al. (2009) Methods for lymphatic vessel culture and gene transfection. *Microcirculation* 16(7):615–628.
47. Hanley CA, Elias RM, Johnston MG (1992) Is endothelium necessary for transmural pressure-induced contractions of bovine truncal lymphatics? *Microvasc Res* 43(2): 134–146.
48. Nizamutdinova IT, et al. (2014) Involvement of histamine in endothelium-dependent relaxation of mesenteric lymphatic vessels. *Microcirculation* 21(7):640–648.
49. Gashev AA (2002) Physiologic aspects of lymphatic contractile function: Current perspectives. *Ann N Y Acad Sci* 979:178–187, discussion 188–196.
50. Scallan JP, Davis MJ (2013) Genetic removal of basal nitric oxide enhances contractile activity in isolated murine collecting lymphatic vessels. *J Physiol* 591(Pt 8):2139–2156.
51. Zweifach BW, Prather JW (1975) Micromanipulation of pressure in terminal lymphatics in the mesentery. *Am J Physiol* 228(5):1326–1335.
52. Benoit JN, Zawieja DC, Goodman AH, Granger HJ (1989) Characterization of intact mesenteric lymphatic pump and its responsiveness to acute edemagenic stress. *Am J Physiol* 257(6 Pt 2):H2059–H2069.
53. Davis MJ, Davis AM, Ku CW, Gashev AA (2009) Myogenic constriction and dilation of isolated lymphatic vessels. *Am J Physiol Heart Circ Physiol* 296(2):H293–H302.
54. Johnston MG, Elias R (1987) The regulation of lymphatic pumping. *Lymphology* 20(4): 215–218.
55. Gashev AA, Davis MJ, Zawieja DC (2002) Inhibition of the active lymph pump by flow in rat mesenteric lymphatics and thoracic duct. *J Physiol* 540(Pt 3):1023–1037.
56. Gashev AA (2008) Lymphatic vessels: Pressure- and flow-dependent regulatory reactions. *Ann N Y Acad Sci* 1131:100–109.
57. Benoit JN (1991) Relationships between lymphatic pump flow and total lymph flow in the small intestine. *Am J Physiol* 261(6 Pt 2):H1970–H1978.
58. Eisenhoffer J, Elias RM, Johnston MG (1993) Effect of outflow pressure on lymphatic pumping in vitro. *Am J Physiol* 265(1 Pt 2):R97–R102.
59. Gashev AA, Delp MD, Zawieja DC (2006) Inhibition of active lymph pump by simulated microgravity in rats. *Am J Physiol Heart Circ Physiol* 290(6):H2295–H2308.
60. Kornuta JA, Brandon Dixon J (2014) Ex vivo lymphatic perfusion system for independently controlling pressure gradient and transmural pressure in isolated vessels. *Ann Biomed Eng* 42(8):1691–1704.
61. Zawieja DC, Davis KL, Schuster R, Hinds WM, Granger HJ (1993) Distribution, propagation, and coordination of contractile activity in lymphatics. *Am J Physiol* 264(4 Pt 2): H1283–H1291.
62. McHale NG, Meharg MK (1992) Co-ordination of pumping in isolated bovine lymphatic vessels. *J Physiol* 450:503–512.
63. Kim SE, Coste B, Chadha A, Cook B, Patapoutian A (2012) The role of *Drosophila* Piezo in mechanical nociception. *Nature* 483(7388):209–212.
64. Bausch AR, Schwarz US (2013) Cellular mechanosensing: Sharing the force. *Nat Mater* 12(11):948–949.
65. Luo T, Mohan K, Iglesias PA, Robinson DN (2013) Molecular mechanisms of cellular mechanosensing. *Nat Mater* 12(11):1064–1071.
66. Humphrey JD, Milewicz DM, Tellides G, Schwartz MA (2014) Cell biology. Dysfunctional mechanosensing in aneurysms. *Science* 344(6183):477–479.
67. Ranade SS, et al. (2014) Piezo1, a mechanically activated ion channel, is required for vascular development in mice. *Proc Natl Acad Sci USA* 111(28):10347–10352.
68. Benoit JN (1997) Effects of alpha-adrenergic stimuli on mesenteric collecting lymphatics in the rat. *Am J Physiol* 273(1 Pt 2):R331–R336.
69. Yokoyama S, Benoit JN (1996) Effects of bradykinin on lymphatic pumping in rat mesentery. *Am J Physiol* 270(5 Pt 1):G752–G756.
70. Davis MJ, et al. (2008) Modulation of lymphatic muscle contractility by the neuropeptide substance P. *Am J Physiol Heart Circ Physiol* 295(2):H587–H597.
71. McNamara GR, Zanetti G (1988) Use of the Boltzmann equation to simulate lattice gas automata. *Phys Rev Lett* 61(20):2332–2335.
72. Schwabl F (2000) *Statistische Mechanik* (Springer, Berlin).
73. Sukop MC, Thorne DT, Jr (2007) Lattice Boltzmann Modeling (Springer, Berlin).
74. Ginzburg I, Verhaeghe F, d'Humieres D (2008) Two-relaxation-time lattice Boltzmann scheme: About parametrization, velocity pressure and mixed boundary conditions. *Commun Comput Phys* 3(2):427–478.
75. Ginzburg I, Verhaeghe F, d'Humieres D (2008) Study of simple hydrodynamic solutions with the two-relaxation-time lattice Boltzmann scheme. *Commun Comput Phys* 3(3):519–581.
76. Dünweg B, Schiller UD, Ladd AJC (2007) Statistical mechanics of the fluctuating lattice Boltzmann equation. *Phys Rev E Stat Nonlin Soft Matter Phys* 76(3 Pt 2):036704.
77. Bhatnagar PL, Gross EP, Krook M (1954) Model for collision processes in gases. I. Small amplitude processes in charged and neutral one-component systems. *Phys Rev* 94(3): 511.
78. Bertram CD, Macaskill C, Moore JE, Jr (2011) Simulation of a chain of collapsible contracting lymphangions with progressive valve closure. *J Biomech Eng* 133(1): 011008.
79. Bertram C, Macaskill C, Moore J, Jr (2013) Incorporating measured valve properties into a numerical model of a lymphatic vessel. *Comput Methods Biomech Biomed Engin* 17(14):1519–1534.